Journal of Neurochemistry
Raven Press, Ltd., New York

Dynamic Measurements of Cerebral Pentose Phosphate Pathway Activity In Vivo Using [1,6-$^{13}C_2$,6,6-$^{2}H_2$]Glucose and Microdialysis

Oded Ben-Yoseph, *Dianne M. Camp, *Terry E. Robinson, and Brian D. Ross

*Departments of Radiology, Biological Chemistry, and *Psychology, University of Michigan, Ann Arbor, Michigan, U.S.A.*

Abstract: Cerebral pentose phosphate pathway (PPP) activity has been linked to NADPH-dependent anabolic pathways, turnover of neurotransmitters, and protection from oxidative stress. Research on this potentially important pathway has been hampered, however, because measurement of regional cerebral PPP activity in vivo has not been possible. Our efforts to address this need focused on the use of a novel isotopically substituted glucose molecule, [1,6-$^{13}C_2$,6,6-$^{2}H_2$]glucose, in conjunction with microdialysis techniques, to measure cerebral PPP activity in vivo, in freely moving rats. Metabolism of [1,6-$^{13}C_2$,6,6-$^{2}H_2$]glucose through glycolysis produces [3-^{13}C]lactate and [3-^{13}C,3,3-$^{2}H_2$]lactate, whereas metabolism through the PPP produces [3-^{13}C,3,3-$^{2}H_2$]lactate and unlabeled lactate. The ratios of these lactate isotopomers can be quantified using gas chromatography/mass spectrometry (GC/MS) for calculation of PPP activity, which is reported as the percentage of glucose metabolized to lactate that passed through the PPP. Following addition of [1,6-$^{13}C_2$,6,6-$^{2}H_2$]glucose to the perfusate, labeled lactate was easily detectable in dialysate using GC/MS. Basal forebrain and intracerebral 9L glioma PPP values (mean ± SD) were 3.5 ± 0.4 (n = 4) and 6.2 ± 0.9% (n = 4), respectively. Furthermore, PPP activity could be stimulated in vivo by addition of phenazine methosulfate, an artificial electron acceptor for NADPH, to the perfusion stream. These results show that the activity of the PPP can now be measured dynamically and regionally in the brains of conscious animals in vivo.
Key Words: Pentose phosphate pathway—Microdialysis—9L gliosarcoma—Brain.
J. Neurochem. **64,** 1336–1342 (1995).

The main functions of the oxidative branch of the pentose phosphate pathway (PPP) are to supply ribose 5-phosphate for nucleotide synthesis and to produce reducing equivalents in the form of NADPH for biosynthetic reactions. The NADPH produced by the PPP also plays an important role in maintaining glutathione in its reduced state. The parameter P, which is defined as the percentage of glucose metabolized to lactate that passes through the PPP, is considered to be relatively small in the brain (~2–8% of the total glucose consumed in rats) (Hostetler and Landau, 1967; Hostetler et al., 1970; Baquer et al., 1975; Gaitonde et al., 1983). However, the fact that P can be stimulated to as much as 80-fold (Baquer et al., 1977; Hothersall et al., 1979) suggests that the PPP has an enormous reserve capacity and indicates that it may play an important role under certain physiological or pathological conditions. For example, the PPP has been suggested to possess a functional significance in various conditions such as the developing (Baquer et al., 1977) and aging (Zubairu et al., 1983) brain and in gliomas (Coleman and Allen, 1978). Studies of excised glioma tissue have reported an increased PPP flux as compared with normal brain (Loreck et al., 1987). In addition, stimulation of PPP activity by catecholamines was demonstrated in isolated synaptosomes (Appel and Parrot, 1970) and whole-brain preparations (Baquer et al., 1977), and a further link to neurotransmission may occur via the aldehydes produced by the catalytic action of monoamine oxidase, which are reduced to their corresponding alcohols by an NADPH-dependent aldehyde reductase (Tabakoff et al., 1974). Baquer et al. (1975) have proposed that the PPP also provides the NADPH utilized by the glutathione pathways for cellular protection from oxidative injury. Oxidative stress can occur during periods where the production of hydrogen peroxide is produced by increased monoamine oxidase activity (Hothersall et al., 1982). Further evidence that a stimulation in PPP activity by monoamine transmitter degradation products is mediated by detoxification of H_2O_2 and the reduction of aldehydes to alcohols in

Received May 10, 1994; revised manuscript received July 21, 1994; accepted August 2, 1994.

Address correspondence and reprint requests to Dr. B. D. Ross at Department of Radiology, University of Michigan, Kresge III, Room R3315, Ann Arbor, MI 48109-0553, U.S.A.

Abbreviations used: GC/MS, gas chromatography/mass spectrometry; MRI, magnetic resonance imaging; P, the percentage of glucose metabolized to lactate that passes through the pentose phosphate pathway; PPP, pentose phosphate pathway; PMS, phenazine methosulfate; TMS, trimethylsilyl.

synaptosomes was provided by Hothersall et al. (1982).

These studies indicate that the cerebral PPP may be of considerable importance in both normal and pathological states. However, at present no method is available to monitor regional brain PPP activity in vivo. Attempts to measure PPP activity in rat brain by quantifying differences in glucose utilization in different brain regions with [1-^{14}C]glucose and [6-^{14}C]glucose have been unsuccessful (Hawkins et al., 1985; Duncan et al., 1988). More recently, Dienel et al. (1992) attempted to measure regional PPP activity by quantifying local rates of glucose utilization, determined with deoxy[1-^{14}C]glucose and deoxy[6-^{14}C]glucose, but concluded that PPP activity in normal adult rat brain was too low to be measured in vivo. An alternate novel approach involves the use of [1,6-$^{13}C_2$,6,6-$^{2}H_2$]-glucose, which was recently reported useful for measuring PPP activity in cultured cells (Ross et al., 1994). In the present report we demonstrate that [1,6-$^{13}C_2$,6,6-$^{2}H_2$]glucose, in combination with intracerebral microdialysis techniques, can also be used to obtain dynamic measurements of regional PPP activity in vivo in the brain and intracerebral 9L gliomas of conscious rats.

MATERIALS AND METHODS

Chemicals

D-[1,6-$^{13}C_2$,6,6-$^{2}H_2$]Glucose was purchased from Omicron Biochemicals (South Bend, IN, U.S.A.). Enrichments of ^{13}C and ^{2}H atoms on the isotopically substituted glucose molecule were determined to be 99 and 98%, respectively, from high-resolution ^{13}C and ^{1}H NMR studies. Bis(trimethylsilyl)trifluoroacetamide was obtained from Alltech Associates (Deerfield, IL, U.S.A.). Cell culture medium was obtained from GIBCO/BRL (Grand Island, NY, U.S.A.). All other chemicals were from Sigma Chemical Co. (St. Louis, MO, U.S.A.).

Cell culture conditions

Rat 9L glioma cells were grown as monolayers in modified Eagle's minimal essential medium containing 10% fetal bovine serum, 100 units/ml of penicillin, and 100 μg/ml of streptomycin. Cells were cultured in an incubator at 37°C in an atmosphere containing 95% air and 5% CO_2. Glioma cells were harvested by trypsinization and concentrated in serum-free medium to yield an intracerebral inoculum dose of 10^5 glioma cells/5 μl.

Induction of brain tumors

Male Fischer rats weighing between 150 and 200 g were used for in vivo brain tumor studies. Rats were anesthetized by an intraperitoneal injection of a mixture containing ketamine (80–100 mg/kg) and xylazine (13 mg/kg). A small incision was made ~3 mm behind the right eye and 2.5 mm from midline. A high-speed drill was used to create a 1-mm-diameter burr hole through the skull. The right forebrain was inoculated with 10^5 cells in 5 μl at a depth of 3 mm. The burr hole was filled with bone wax to minimize the potential for extracerebral extension of the tumor tissue. The skin was sutured, and the rats were allowed to recover. Between 18 and 22 days postimplantation, rats with glioma cell implants underwent examination by magnetic resonance imaging (MRI) for assessment of tumor size and location for subsequent placement of the microdialysis probe.

MRI

In vivo magnetic resonance experiments were performed on a Spectroscopy Imaging Systems Corp. (SISCO) imaging spectrometer system equipped with a 7.0-Tesla, 18.3-cm horizontal-bore magnet. Animals were maintained at 37°C using a circulating water blanket placed under the torso. The rat's head was positioned inside a 5-cm-diameter birdcage radiofrequency coil and placed inside the center of the magnet. Each MRI session included (a) single-slice gradient-recalled-echo scanning with 1-mm "saturation cross-hairs" imprinted on the axial and coronal images to facilitate rapid positioning of the coil and (b) a T_2-weighted (TR/TE = 3,000/60 ms) 20-slice scan through the brain (1 mm slice thickness, 128 × 128 matrix) for determination of the size and location of the tumor to guide subsequent implantation of microdialysis probes.

Construction and implantation of microdialysis probes

Concentric-style microdialysis probes were similar to those described by Robinson and Camp (1991) with the following modifications. The inlet and outlet tubing consisted of fused silica capillary tubing (inlet, 150 μm o.d., 75 μm i.d.; outlet, 170 μm o.d., 100 μm i.d.). The regenerated cellulose hollow dialysis fiber had an effective length of 6 mm and extended from the surface of the dura to 6 mm ventral. The dialysis fiber had a nominal molecular mass cut-off of 5,000–6,000 Da, an i.d. of 215 μm, and a wall thickness of 18 μm (o.d. = 251 μm).

Male Fischer rats weighing 250–350 g were injected with 0.15 ml of atropine methylnitrate (0.5 mg/ml) and then anesthetized with sodium pentobarbital. A 21-ga stainless steel guide cannula was placed on the dural surface using standard stereotactic techniques. The coordinates used (with bregma horizontal to λ) were 0.6 mm anterior to bregma, 3.6 mm lateral from the midline, and 1.0 mm from the skull surface. The guide cannula was then fixed to the skull using jeweler's screws and cranioplast dental cement. A 26-ga stylet protruded 1 mm beyond the tip of the cannula to maintain patency. Animals were allowed to recover for 6–7 days before probe implantation. One day before a dialysis experiment, the dialysis probe was attached to a liquid swivel, which in turn was connected to a gas-tight Hamilton syringe mounted on a syringe pump, and the perfusion solution was pumped through the probe at 0.3 μl/min. The dialysis probe was then lowered into the implanted guide cannula. The animals were attached to the liquid swivel via a tether connected to a piece of stainless steel tubing mounted to the dental acrylic cap and placed into test chambers. The perfusion solution, which was filter-sterilized, consisted of 145 m*M* NaCl, 2.7 m*M* KCl, 1.3 m*M* $CaCl_2$, 1.0 m*M* $MgCl_2$, and 0.2 m*M* ascorbic acid, pH 7.3. On the day of the experiment, the perfusion solution was replaced with fresh solution containing 100 m*M* [1,6-$^{13}C_2$,6,6-$^{2}H_2$]glucose, and the flow rate was adjusted to 1.0 μl/min. After a 60-min equilibration period, dialysate samples were continuously collected in polyethylene tubes at 50-min intervals over the experimental period.

For animals with intracranial 9L tumors, MRI was performed 2 days before microdialysis experiments to determine the size and location of the tumor within the brain paren-

chyma. Surgical attachment of guide cannulas for tumor-bearing rats was carried out as described above, and animals were allowed to recover for 1–2 days. Probes were typically implanted 1 mm posterior to the tumor injection site, which was essentially the same site as for controls.

Microdialysis equilibration studies

To determine the dynamics and extent of incorporation of the label from labeled glucose to lactate, microdialysis experiments were performed on normal rat brains using [1-^{13}C]glucose in the perfusion stream. Rats (n = 3 per group) with implanted dialysis probes were perfused with [1-^{13}C]-glucose at a concentration of 10, 50, 75, 100, or 150 m*M*, and samples were collected every 20 min. The [1-^{13}C]glucose solutions were added and removed at 20 and 200 min, respectively, following initiation of sample collection. Dialysis samples were collected for a total of 260 min. Lactate fractional enrichment was calculated using the *m/z* 219 and 220 ions obtained from gas chromatography/mass spectrometry (GC/MS) analysis.

GC/MS analysis

All GC/MS measurements were performed as previously described (Ross et al., 1994). In brief, samples were lyophilized to dryness and derivatized by adding 50 μl of pyridine and 50 μl of (trimethylsilyl)trifluoroacetamide and heating for 15 min at 60°C. The samples were then centrifuged at 12,000 *g* for 10 min. The supernatant was pipetted off and placed into a vial, which was then sealed with a Teflon-coated septum. The trimethylsilyl (TMS) derivative was chosen over other possible derivatives because of the ease of derivatization, its characteristic fragment ions, and its gas chromatographic separation from interfering compounds. An HP 5890/5971 GC/MS system with an HP DB-5 fused silica column (30 m × 0.25 mm × 0.25 μm) with helium as the carrier gas was used. Dwell time was 20 ms, and electron multiplier voltage during acquisition was 2,280 V. The column temperature program was 0.75 min at 55°C followed by a temperature ramp at 15°C/min to 140°C. The temperature was then increased to 280°C at 30°C/min and held for 3 min. Selected ion monitoring was performed on the *m/z* 219, 220, 221, and 222 ions, which correspond predominately to unlabeled lactate, [3-^{13}C]lactate, [3-^{13}C,3-^{2}H]-lactate, and [3-^{13}C,3,3-^{2}H$_2$]lactate, respectively (Ross et al., 1994). These ions correspond to the loss of a methyl group from the TMS derivative of lactic acid. Under these chromatographic conditions the lactate peak was well resolved with no interfering peaks.

In vitro isotopic dilution studies

In the TMS derivative of lactate, each atom contains several naturally occurring isotopes. With this silylated derivative, ~20% of the *m/z* 219 ion is found in the M+1 (*m/z* 220) ion owing to naturally occurring isotopes of carbon and silicon. When the amount of labeled lactate is low, quantification of the [3-^{13}C]lactate in the *m/z* 220 ion can become difficult, resulting in an incorrectly calculated PPP activity. This could potentially become significant for in vivo microdialysis studies because of the presence of unlabeled blood glucose and other sources of endogenous unlabeled lactate precursors. To determine the relative amount of unlabeled lactate, which would affect the accurate quantification of labeled lactate and ultimately the calculation of accurate PPP activities, isotopic dilution studies were undertaken using 9L glioma cultures. For these studies, [1,6-^{13}C$_2$,6,6-^{2}H$_2$]glucose was diluted from 100 to 10% in 10% steps while maintaining the total concentration of glucose constant at 5.5 m*M* in Krebs–Ringer's buffer. Incubations were performed in 24-well culture plates for 30 min, and each concentration was replicated using four wells for statistical analysis.

Calculation of PPP activity

The GC/MS intensities were adjusted for their natural isotopic composition and resolved into [C1]lactate and [C6]lactate components originating from the C1 and C6 positions of glucose, respectively. The PPP activity is calculated using the following equation as previously described (Ross et al., 1994): P = 1 − [C1]lactate/[C6]lactate. A small adjustment can be made to compensate for recycling of glucose 6-phosphate through the PPP (Ross et al., 1994).

Figure 1 shows the labeling patterns of metabolites of glycolysis and the PPP when [1,6-^{13}C$_2$,6,6-^{2}H$_2$]glucose is used as precursor. Metabolism of [1,6-^{13}C$_2$,6,6-^{2}H$_2$]glucose through the glycolytic pathway to lactate results in the formation of [3-^{13}C]lactate (*m/z* = 220) and [3-^{13}C,3,3-^{2}H$_2$]-lactate (*m/z* = 222), from the C1 and C6 positions of glucose, respectively. In contrast, metabolism of [1,6-^{13}C$_2$,6,6-^{2}H$_2$]glucose through the oxidative pathway of the PPP results in a loss of label from the C1 position of glucose as $^{13}CO_2$ due to the decarboxylation of 6-phosphogluconate by the catalytic action of phosphogluconate dehydrogenase. Labeling of sugars in the nonoxidative part of the PPP will thus appear in the C5 position of ribose 5-phosphate and xylulose 5-phosphate, the C7 position of sedoheptulose 7-phosphate, the C4 position of erythrose 4-phosphate, the C3 position of glyceraldehyde 3-phosphate, and the C6 position of fructose 6-phosphate. Reentry of glyceraldehyde 3-phosphate and fructose 6-phosphate derived from the PPP into glycolysis results in the production of [3-^{13}C,3,3-^{2}H$_2$]lactate (*m/z* = 222) and unlabeled lactate (*m/z* = 219). The activity of the PPP can be calculated as described above using the lactate isotopomer values obtained from GC/MS analysis.

RESULTS AND DISCUSSION

In vitro isotopic dilution studies

The TMS derivative of unlabeled lactate (*m/z* = 219) contains a significant isotopic tail that contributes 19.4, 8.9, and 1.2% of its area to the *m/z* = 220, 221, and 222 labeled lactate species, respectively. In vitro incubation studies were undertaken to determine the amount of unlabeled lactate at which quantification of the labeled lactate in the *m/z* 220 peak becomes difficult. Glioma cells were incubated with increasing dilutions of [1,6-^{13}C$_2$,6,6-^{2}H$_2$]glucose with unlabeled glucose, and the activity of the PPP was determined. A relatively constant value of basal PPP activity was obtained when the proportion of [1,6-^{13}C$_2$,6,6-^{2}H$_2$]-glucose in the medium was ≥30% (Fig. 2). Accurate PPP values were obtained down to 20% fractional enrichment of glucose, at which point the uncorrected (*m/z* 219)/(*m/z* 220) ratio was 3.5. To allow a margin of safety, it is suggested that the ratio of (*m/z* 219)/(*m/z* 220) should be kept below ~3.0 (at 30% labeled glucose). A similar pattern was observed at the upper range of PPP activity during stimulation with 50 μ*M* PMS. This point is of importance because microdia-

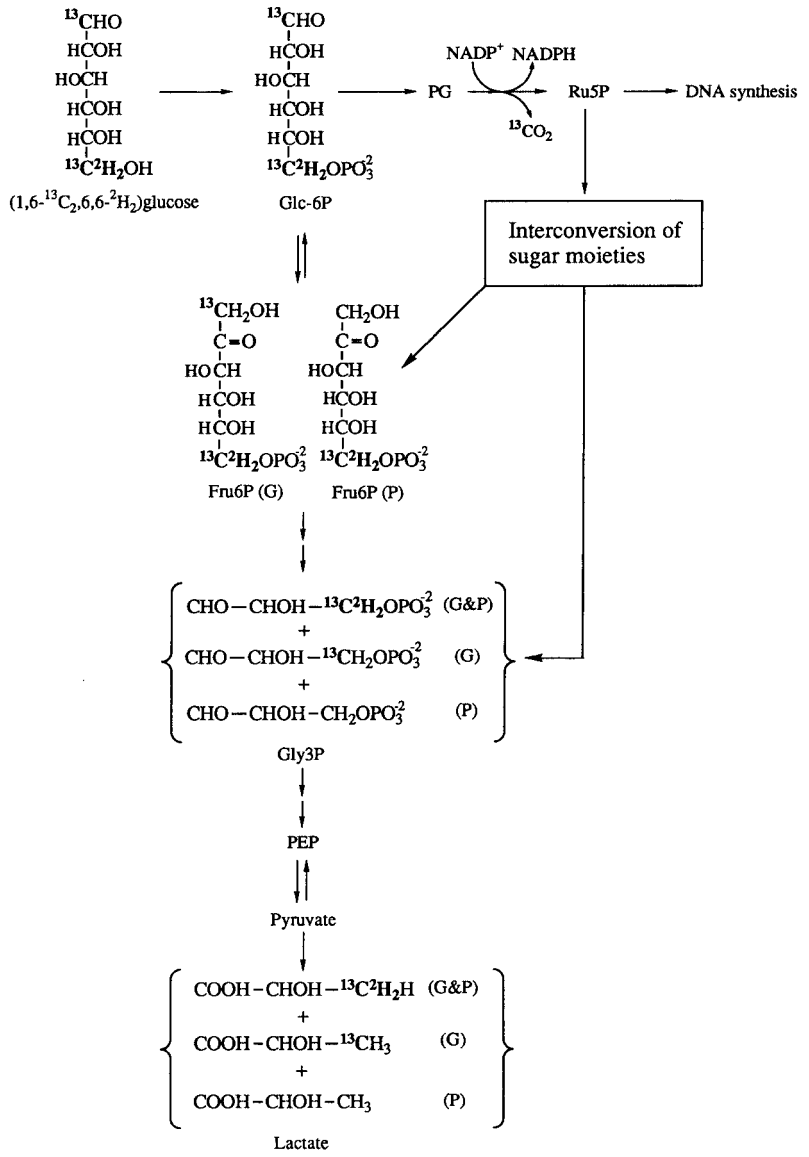

FIG. 1. The fate of [1,6-$^{13}C_2$,6,6-$^{2}H_2$]-glucose through glycolysis and the pentose phosphate pathway (PPP). Interconversion of sugar moieties refers to the nonoxidative branch of the PPP. G and P indicate the origin of a metabolite from glycolysis or PPP. Glc-6P, glucose 6-phosphate; PG, phosphogluconate; Ru5P, ribulose 5-phosphate; Fru6P, fructose 6-phosphate; Gly3P, glyceraldehyde 3-phosphate; PEP, phosphoenolpyruvate.

lysis measurements of in vivo PPP will have significant contributions of unlabeled lactate from metabolism of unlabeled glucose in the blood, which would be metabolized along with [1,6-$^{13}C_2$,6,6-$^{2}H_2$]glucose in the perfusion stream. If the (m/z 219)/(m/z 220) ratio of 3–3.5 cannot be achieved owing to the presence of high levels of unlabeled lactate precursors, it may be possible to obtain useful data by using the n-propyl heptafluorobutyrate derivative of lactate (Tserng et al., 1984).

Microdialysis equilibration studies

To determine the dynamics of lactate enrichment and washout following a change in the amount of labeled glucose in the perfusion stream, [1-^{13}C]glucose was added to the perfusion stream at 10, 50, 75, or 100 mM, and the percent enrichment in lactate was determined over time. Because only half of the lactate produced from this glucose is labeled, the fractional enrichment would be approximately doubled if [1,6-$^{13}C_2$,6,6-$^{2}H_2$]glucose was used. The [1-^{13}C]glucose was added at 20 min following initiation of experiments and was removed at 200 min. The percent enrichment of lactate increased for 40 min following addition of [1-^{13}C]glucose and plateaued until [1-^{13}C]-glucose was replaced by unlabeled glucose (Fig. 3). Maximal enrichments of ~25% were achieved within 40 min after administration of 75, 100, and 150 mM (data not shown) [1-^{13}C]glucose. A similar pattern was observed with 50 mM [1-^{13}C]glucose with a slightly lower maximal fractional enrichment of 22%. With 10 mM [1-^{13}C]glucose in the perfusion solution, maximal enrichment reached only 11%. These results indicate that an equilibration period of at least 40 min

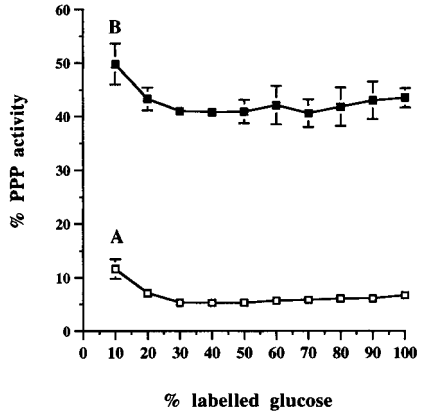

FIG. 2. PPP activity in cultured 9L glioma cells with different mole fractions of [1,6-$^{13}C_2$,6,6-$^{2}H_2$]glucose during a 30-min incubation period. Total glucose concentrations were maintained at 5.5 m*M* for all enrichment conditions. PPP activity was determined under (**A**) basal conditions and (**B**) in the presence of 50 μM PMS. Data are mean ± SD (bars) values (n = 4).

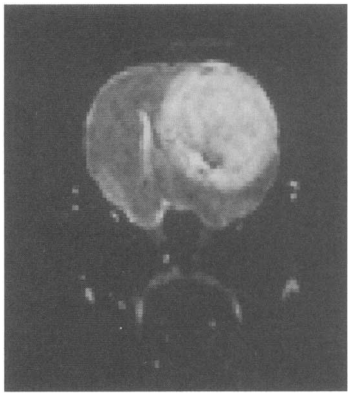

FIG. 4. Representative coronal T_2-weighted (*TR*/*TE* = 3,000/60, slice thickness = 0.5 mm) magnetic resonance image of an intracranial 9L glioma in the forebrain of a rat used for placement of dialysis probe. The tumor is evident as a large hyperintense region in the right hemisphere.

was required for labeling to reach a plateau. The results shown in Fig. 3 also indicate that increasing the amount of labeled glucose in the perfusion stream to >75 m*M* will not significantly increase the amount of labeled lactate. Once the labeled glucose was withdrawn from the perfusion stream, a similar duration was required for label washout.

The fractional enrichment of lactate did not increase when the glucose concentration was increased to >75 m*M* [1-^{13}C]glucose. At 50 m*M* [1-^{13}C]glucose, however, the fractional enrichment was slightly but significantly lower. This suggests that glucose carrier saturation occurs between these two concentrations. Assuming that glucose transport becomes saturated at ~20 m*M* (Bachelard et al., 1973) and that the normal concentration of unlabeled brain glucose is 5 m*M*, it appears that ~15 m*M* glucose diffused from the perfusion solution through the dialysis probe when 75 m*M* [1-^{13}C]glucose was present in the perfusion solution. This corresponds to ~20% diffusion of glucose across the dialysis probe membrane.

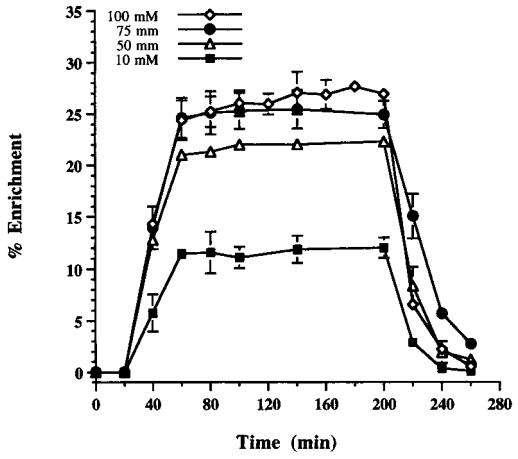

FIG. 3. GC/MS measurements of lactate fractional enrichment in the dialysate collected from rat forebrain versus time following addition and removal of [1-^{13}C]glucose to the perfusion stream at 20 and 200 min, respectively. Samples were collected at 20-min intervals following perfusion with 10, 50, 75, or 100 m*M* [1-^{13}C]glucose in the perfusion solution. Data are mean ± SD (bars) values (n = 3).

Measurements of PPP activity in brain and in solid tumor

Magnetic resonance images of the brain were acquired to ensure proper placement of dialysis probes into intracranial 9L gliomas. A representative T_2-weighted image of an intracranial 9L glioma is shown in Fig. 4. The glioma is clearly delineated in the right hemisphere as a large hyperintense region. Selective collection of dialysates from the intracranial gliomas was easily achieved by preimaging the brains so that the proper location and depth of the dialysis probe could be determined for individual tumors.

The PPP activity in brain and glioma was measured over 50-min intervals using 100 m*M* [1,6-$^{13}C_2$,6,6-$^{2}H_2$]glucose in the perfusion stream, and the results are shown in Fig. 5. Basal activity in normal brain was 3.5 ± 0.4% (mean ± SD, n = 4), which is in agreement with studies by Hostetler and Landau (1967), who reported PPP activity of 3–5% in whole rat brain extracts following administration of [2-^{14}C]-glucose. Lower values between 0.5 and 2.5% have also been reported using other cerebral preparations (Coleman and Allen, 1978; Hothersall et al., 1979; Bauer and Brand, 1982).

It has been reported previously that PPP activity is significantly elevated in tumor tissue. For example, values of 7.5 ± 1.5 and 5.1 ± 1.2% were obtained in C6 and 9L glioma cultures, respectively (Kingsley-Hickman et al., 1990). Similarly, in the present study, basal PPP activity in 9L glioma tissue in vivo was 6.2

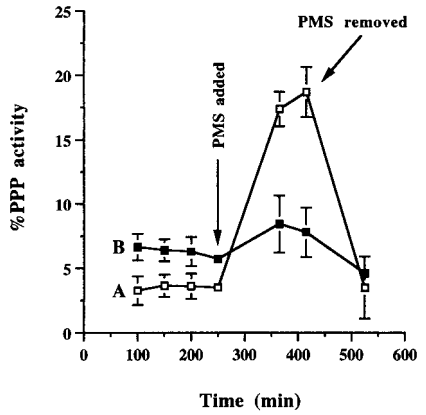

FIG. 5. PPP activity in the forebrain and 9L glioma of conscious rats versus time. Samples were collected at 50-min intervals. Stimulation of the PPP to 18.7 ± 1.9 and 8.4 ± 1.1% was observed for (line A) normal brain (□) and (line B) tumor (■), respectively, following addition of 50 μ*M* PMS to the perfusion solution at 250 min. Recovery of PPP activity to basal levels occurred over time following removal of PMS at 400 min. Data are mean ± SD (bars) values.

± 0.9% (mean ± SD, n = 4), which is significantly higher than observed in normal cerebral tissue (Fig. 5). The higher basal PPP activity of the 9L glioma compared with normal brain is probably associated with an elevated NADPH requirement necessary for the increased nucleic acid, steroid, and lipid biosynthesis of the proliferating neoplasm.

Glucose 6-phosphate dehydrogenase is the sole regulatory enzyme of the pathway, and the activity is modulated by the NADPH/$NADP^+$ ratio. For this reason compounds that are metabolized via NADPH-consuming pathways will cause PPP stimulation, whereas compounds that block NADPH utilization will inhibit the pathway (Fabregat et al., 1985). Phenazine methosulfate (PMS), an electron acceptor for NADPH, is known to reduce the NADPH/$NADP^+$ ratio (Dickens and McIlwain, 1938), thus pulling the glucose 6-phosphate dehydrogenase equilibrium toward 6-phosphogluconate production. Addition of 50 μ*M* PMS to the perfusion solution at 250 min after [1,6-$^{13}C_2$,6,6-$^2H_2$]-glucose administration resulted in stimulation of the pathway to 18.7 ± 1.9% in brain and to 8.4 ± 1.1% in tumor (Fig. 5). PPP activity returned to basal levels following removal of PMS from the perfusion solution at 400 min. The exact reasons for the apparent increased stimulation of brain PPP compared with glioma at dialysate concentrations of 50 μ*M* PMS are outside the scope of this present study and remain a topic for further research. Under these experimental conditions, the lactate (*m/z* 219)/(*m/z* 220) ratio of dialysis samples was 1.5, which is acceptable for accurate quantification of PPP activity.

Finally, in pilot experiments (data not shown) dialysate samples were collected in 10-min intervals to determine the potential temporal resolution of this method. It was found that with 50 m*M* [1,6-$^{13}C_2$,6,6-$^2H_2$]glucose in the perfusion stream PPP activity could be easily monitored over ≤10-min intervals. Furthermore, with 50 m*M* glucose, the lactate (*m/z* 219)/(*m/z* 220) ratio was 1.8, suggesting that it should be feasible to decrease further the concentration of [1,6-$^{13}C_2$,6,6-$^2H_2$]glucose in the perfusion stream.

In conclusion, the results reported here indicate that [1,6-$^{13}C_2$,6,6-$^2H_2$]glucose can be used to quantify regional PPP activity in the brain of conscious rats when coupled with microdialysis techniques. This method allows sampling of discrete brain regions with reasonable temporal resolution, and it should be practical to monitor PPP activity under various physiological, behavioral, or pathological conditions. This novel method should facilitate further studies of the role of the PPP in the CNS.

Acknowledgment: We would like to thank Dr. Peter B. Kingsley for helpful comments. This work was supported in part by the following grants: BE-149 from the American Cancer Society, R29 CA59009 and P20 NS31114-01 from the National Institutes of Health, and 04294 from the National Institute on Drug Abuse. O. B.-Y. is the recipient of a fellowship from the American Brain Tumor Association. GL tumor cells were provided by the Brain Tumor Research Center at U.C. San Francisco.

REFERENCES

Appel S. H. and Parrot B. L. (1970) Hexosemonophosphate pathway in synapses. *J. Neurochem.* **17,** 1619–1626.

Bachelard H. S., Daniel P. M., Love E. R., and Pratt O. E. (1973) The transport of glucose into the brain of the rat *in vivo*. *Proc. R. Soc. Lond.* [*Biol.*] **183,** 71–82.

Baquer N. Z., McLean P., and Greenbaum A. L. (1975) Systems relationships and the control of metabolism pathways in developing brain, in *Normal and Pathological Development of Energy Metabolism* (Hommes F. A. and Van den Berg C. J., eds), pp. 109–132. Academic Press, London.

Baquer N. Z., Hothersall J. S., McLean P., and Greenbaum A. L. (1977) Aspects of carbohydrate metabolism in developing brain. *Dev. Med. Child Neurol.* **19,** 81–104.

Bauer U. and Brand K. (1982) Carbon balance studies of glucose metabolism in rat cerebral cortical synaptosomes. *J. Neurochem.* **39,** 239–243.

Coleman M. Y. and Allen N. (1978) The hexose monophosphate pathway in ethylnitrosourea induced tumors of the nervous system. *J. Neurochem.* **30,** 83–90.

Dickens F. and McIlwain H. (1938) Phenazine compounds as carriers in the hexose-monophosphate system. *Biochem. J.* **32,** 1615–1625.

Dienel G. A., Cruz N. F., Nakanishi H., Melzer P., Moulis P., and Sokoloff L. (1992) Comparison of rates of local cerebral glucose utilization determined with deoxy[1-^{14}C]glucose and deoxy[6-^{14}C]glucose. *J. Neurochem.* **59,** 1430–1436.

Duncan G. E., Stumpf W. E., Brustle O., Givens B. S., Breese G. R., and Pilgrim C. (1988) Topography of basal glucose utilization in the hippocampus determined with [1-^{14}C]glucose and [6-^{14}C]glucose. *Neuroscience* **24,** 877–883.

Fabregat I., Vitorica J., Satrustegui J., and Machado A. (1985) The pentose phosphate cycle is regulated by NADPH/NADP ratio in rat liver. *Arch. Biochem. Biophys.* **236,** 110–118.

Gaitonde M. K., Evison E., and Evans G. M. (1983) The rate of utilization of glucose via hexosemonophosphate shunt in brain. *J. Neurochem.* **41,** 1253–1260.

Hawkins R. A., Mans A. M., Davis D. W., Vina J. R., and Hibbard L. S. (1985) Cerebral glucose use measured with [^{14}C]glucose labeled in the 1, 2 or 6 position. *Am. J. Physiol.* **248,** C170–C176.

Hostetler K. Y. and Landau B. R. (1967) Estimation of the pentose cycle contribution to glucose metabolism in tissue *in vivo*. *Biochemistry* **6,** 2961–2964.

Hostetler K. Y., Landau B. R., White R. J., Albin M. S., and Yashon D. (1970) Contribution of the pentose cycle to the metabolism of glucose in the isolated, perfused brain of the monkey. *J. Neurochem.* **17,** 33–39.

Hothersall J. S., Baquer N. Z., Greenbaum N. L., and McLean P. (1979) Alternative pathways of glucose utilization in brain: changes in the pattern of glucose utilization in brain during development and the effects of phenazine methosulfate on the integration of metabolic routes. *Arch. Biochem. Biophys.* **198,** 478–492.

Hothersall J. S., Greenbaum A. L., and McLean P. (1982) The functional significance of the pentose phosphate pathway in synaptosomes: protection against peroxidative damage by catecholamines and oxidants. *J. Neurochem.* **39,** 1325–1332.

Kingsley-Hickman P. B., Ross B. D., and Krick T. (1990) Hexose monophosphate shunt measurement in cultured cells with (1-^{13}C)glucose: correction for endogenous carbon sources using (6-^{13}C)glucose. *Anal. Biochem.* **185,** 235–237.

Loreck D. J., Galarraga J., Van der Feen J., Phang J. M., Smith B. H., and Cummins C. J. (1987) Regulation of the pentose phosphate pathway in human astrocytes and gliomas. *Metab. Brain Dis.* **2,** 31–46.

Robinson T. E. and Camp D. (1991) The feasibility of repeated microdialysis for within subjects design experiments: studies on the mesostriatal dopamine system, in *Microdialysis in the Neurosciences. Techniques in the Behavioral and Neural Sciences, Vol. 7* (Robinson T. E. and Justice J. B. Jr., eds), pp. 189–234. Elsevier, Amsterdam.

Ross B. D., Kingsley P. B., and Ben-Yoseph O. (1994) Measurement of pentose phosphate pathway activity in a single incubation with, [1,6-$^{13}C_2$,6,6-$^{2}H_2$] glucose. *Biochem. J.* **302,** 31–38.

Tabakoff B., Groskopt W., Anderson R., and Alivisatos S. G. A. (1974) Biogenic aldehyde metabolism, relation to pentose shunt in brain. *Biochem. Pharmacol.* **23,** 1710–1719.

Tserng K.-Y., Gilfillan C. A., and Kalhan S. C. (1984) Determination of carbon-13 labeled lactate in blood by gas chromatography/mass spectrometry. *Anal. Chem.* **56,** 517–523.

Zubairu S., Hothersall J. S., El-Hassan A., McLean P., and Greenbaum L. (1983) Alternative pathways of glucose utilization in brain: changes in the pattern of glucose utilization and of the response of the pentose phosphate pathway to 5-hydroxytryptamine. *J. Neurochem.* **41,** 76–83.